

Article

Combined Small RNA and Degradome Sequencing Reveals Important Roles of Light-Responsive microRNAs in Wild Potato (*Solanum chacoense*)

Yan Qiao ^{1,2,*} , Fang Yang ¹, Qian Li ¹, Panrong Ren ^{1,3}, Peipei An ^{1,3}, Dan Li ¹ and Junfei Xiao ⁴¹ College of Agriculture and Forestry, Longdong University, Qingyang 745000, China² Gansu Key Laboratory of Protection and Utilization for Biological Resources and Ecological Restoration, Longdong University, Qingyang 745000, China³ Collaborative Innovation Center for Longdong Dryland Crop Germplasm Improvement & Industrialization, Longdong University, Qingyang 745000, China⁴ Gansu Key Laboratories of Crop Improvement & Germplasm Enhancement and Aridland Crop Science, Gansu Agricultural University, Lanzhou 730070, China

* Correspondence: yanqiao@ldxy.edu.cn; Tel.: +86-15097118671

Abstract: The accumulation of chlorophyll and antinutritional glycoalkaloids in potato tubers resulting from exposure to light has been widely recognized as a cause of unpredictable quality loss of potato tuber. While transcriptional regulation of light-induced chlorophyll and glycoalkaloids accumulation has been extensively investigated, the mechanisms of post-transcriptional regulation through miRNA remain largely unexplored. An experimental model, the tubers of *Solanum chacoense*, were used to identify light-responsive miRNA–target interactions (MTIs) related to tuber greening and glycoalkaloid biosynthesis by employing multi-omics approaches (miRNA-seq and degradome-seq). A total of 732 unique mature miRNAs have been identified in *S. chacoense*. In total, 6335 unique target transcripts were cleaved by 489 known miRNAs and 153 novel miRNAs. The results revealed that light-responsive miRNAs can be grouped into eight temporally related clusters and play important roles in various physiological processes such as plant growth, stress responses, and primary and secondary metabolism. Multi-omics analyses have revealed that the modulation of transcript abundance of *MYB59*, *HSPs*, and *EBF1/EBF2* by light-responsive miRNAs is pivotal for their function in cross-tolerance responses to both abiotic and biotic stresses. Furthermore, our findings suggest that many light-responsive miRNAs are crucial regulators in various biosynthetic pathways, including tetrapyrrole biosynthesis, suberin biosynthesis, and steroid biosynthesis. These findings highlight the significant role of light-responsive miRNAs in secondary metabolic pathways, particularly in isoprenoid, terpenoid, and glycoalkaloid biosynthesis, and have implications for the precise manipulation of metabolic pathways to produce new potato varieties with improved resistance to greening and lower glycoalkaloid levels.

Keywords: *Solanum chacoense*; light-responsive microRNAs; high-throughput sequencing; miRNA-target interactions; steroidal glycoalkaloids



Citation: Qiao, Y.; Yang, F.; Li, Q.; Ren, P.; An, P.; Li, D.; Xiao, J. Combined Small RNA and Degradome Sequencing Reveals Important Roles of Light-Responsive microRNAs in Wild Potato (*Solanum chacoense*). *Agronomy* **2023**, *13*, 1763. <https://doi.org/10.3390/agronomy13071763>

Academic Editors: Tatjana Gavrilenko and Alex V. Kochetov

Received: 9 May 2023

Revised: 26 June 2023

Accepted: 27 June 2023

Published: 29 June 2023



Copyright: © 2023 by the authors. Licensee MDPI, Basel, Switzerland. This article is an open access article distributed under the terms and conditions of the Creative Commons Attribution (CC BY) license (<https://creativecommons.org/licenses/by/4.0/>).

1. Introduction

Potato (*Solanum tuberosum* L.) is the world's third most crucial crop for direct human consumption, providing vital nutrients, energy, and vitamins. Over recent decades, potato cultivation has played a crucial role in enhancing food security, improving farmer income, and diversifying diets in numerous countries [1]. Potato tubers are subterranean stems filled with amyloplasts that lack chlorophyllous pigments [2]. However, exposure to light during growth and post-harvest stages can result in a significant increase in tuber chlorophyll, as well as the accumulation of toxic steroidal glycoalkaloids (SGAs) in the periderm, affecting perceived taste and food safety [3–5]. Tuber greening and high glycoalkaloid

accumulation can lead to unpredictable quality loss of potato tubers during supply chain operations. Moreover, tuber greening and glycoalkaloid accumulation can be influenced by genetic factors, tuber physiology, and environmental factors [3,6]. However, the possible mechanisms of light-induced tuber chlorophyll and glycoalkaloid accumulation remain to be elucidated.

Gene regulatory networks are responsible for regulating the biosynthesis of chlorophyll and SGAs in potato tubers. Considering the light-dependent pathway involved, it is not surprising that exposure to light can efficiently promote tuber greening and SGAs biosynthesis at the epigenetic [7], transcriptional [8,9], and post-transcriptional levels [10]. Epigenetic modifications, such as DNA methylation, play a crucial role in regulating potato tuber greening in response to light [7]. Emerging evidence implicates altered genome-wide DNA methylation during the greening of postharvest potatoes [7]. Furthermore, light-induced methylated genes in potato tubers have been confirmed to be associated with starch biosynthesis, chlorophyll synthesis, and gibberellic acid signaling [7]. Remarkably, light can easily modulate the DNA methylation status of noncoding regions in potato tubers. Light-induced tuber greening involves biological processes related to chloroplast development and chlorophyll biosynthesis. Previous research has identified at least 15 enzymes involved in chlorophyll biosynthesis, starting from glutamyl-tRNA to Chl a and Chl b [11]. Transcriptional regulation of these enzymes is essential for chlorophyll accumulation in plants. As one of the most important abiotic factors, light provides the energy source for plant development and physiological responses [12]. To optimize light absorption, plants have evolved sophisticated photoreceptor systems that can perceive various wavelengths of light [13]. In potato, PhyA and PhyB participate in the biosynthesis of chlorophylls [14], with PhyB positively controlling chlorophyll and glycoalkaloid biosynthesis in response to red light [6]. Light of different wavelengths has varying effects on chlorophyll and glycoalkaloids biosynthesis [15,16]. Notably, red light is a crucial factor affecting the biosynthesis of glycoalkaloids and chlorophyll in potato [15,16], leading to the positive elevation of calmodulin and G protein levels in potato tuber, which can activate steroidal alkaloids genes through PhyB-mediated light signaling pathways [17]. In addition, suberin, an extracellular lipid-based barrier found in various land-plant tissues, is involved in defending against abiotic and biotic stresses [18,19]. *CYP86A33*, a gene related to suberin biosynthesis in potato tuber periderm, conferring physiological resistance to potato tuber greening [20].

In recent years, tremendous progress has been made in solanaceae genetics and genomics, and numerous steroidal alkaloids gene have been identified [8,21]. A large-scale co-expression analysis between potato and tomato revealed that many genes are co-expressed with known steroidal alkaloid genes, and at least 10 genes participate in the biosynthesis of steroidal alkaloids [8]. In potato, four steroidal alkaloid genes, including two *UDP-GLYCOSYLTRANSFERASES* (*SGT1*, *SGT3*), the *2-OXOGLUTARATE-DEPENDENT DIOXYGENASE*, and the *CYP72* gene *GAME6*, are clustered on chromosome 7. The transaminase *GAME12* and the *CYP88D* gene *GAME4* are closely located on chromosome 12 [8]. Together, these genes are responsible for the biosynthesis pathway that converts cholesterol to steroidal alkaloids through hydroxylation, oxidation, and transamination reactions.

Transcriptional regulatory information related to tuber green and glycoalkaloid biosynthesis in potato has been revealed, but the roles of miRNAs in these processes are still unclear. MiRNAs are known to play critical roles in post-transcriptional gene regulation, fine-tuning primary and secondary metabolism by targeting key metabolic enzymes [22,23]. Notably, miRNAs can influence chlorophyll biosynthesis and secondary metabolism via light-dependent pathways. In rice, 32 differentially expressed miRNAs were found to play an important role in PhyB-mediated light signaling [24], and miR172, which is regulated by PhyB, plays a crucial role in chlorophyll biosynthesis [24,25]. Light-responsive miRNAs have also been observed to target *bZIP* and *bHLH* transcription factors in potato alkaloid metabolism [10]. *SPL9*, one of miR156 targets, negatively modulated anthocyanin biosynthesis in *Arabidopsis*. Moreover, miRNAs regulated plant metabolism. In *Arabidopsis*,

miR163 and pri-miR163 were up-regulated by light, which targeted *PXMT1* encoded a gene related to hormone methylation and promoted root growth [23]. Nutrient allocation plays an important role in metabolism. The copper element is one of the key factors in photosynthesis; additionally, *SPL7* is regulated by miR408 and is helpful in maintaining copper homeostasis [23]. In addition, miR482b-3p has been found to modulate potato glycoalkaloid biosynthesis by targeting uridine kinase, and the miR479/*CYTOCHROME P450* module can participate in glycoalkaloid biosynthesis in potato [10]. These findings suggest that miRNAs can affect the biosynthesis of chlorophyll and glycoalkaloids through light-signaling pathways, although our understanding of how miRNAs mediate light signaling in potato remains limited. Therefore, it is essential to clarify the miRNA-target interactions (MTIs), and degradome sequencing (degradome-seq) is an effective way to identify mRNA cleavage sites that map onto miRNA targets [26,27]. By integrating miRNA-seq and degradome sequencing, we can accelerate our understanding of the roles of miRNAs in potato tuber green and glycoalkaloids biosynthesis.

In this study, we investigated the potential biological function of miRNAs in *S. chacoense* to respond to light stress. We performed high-throughput miRNA-seq and degradome-seq on tubers of *S. chacoense* control plants and plants induced by light. Based on the degradome sequencing data, the targets were further validated by target plot (t-plot). Overall, this study sheds light on the potential roles of miRNAs in regulating plant responses to light stress and highlights their importance in primary and secondary metabolism in *S. chacoense*.

2. Materials and Methods

2.1. Plant Material and Treatment

S. chacoense is a wild potato species that contains high levels of steroidal glycoalkaloids in its tubers, making it an ideal experimental model for studying the function of SGAs in the natural chemical defense system [28]. The plantlets of *S. chacoense* were propagated in vitro on Murashige and Skoog (MS) medium [29]. Plantlets were cultured at a temperature of 22 °C under long-day (LD) conditions consisting of 16-h light and 8-h dark cycles. Dark-grown plantlets were collected as the control group. To induce tuber formation, 40-day-old plantlets were transferred to a growth chamber under short-day conditions at a temperature of 20 °C. These plantlets were grown in the dark for three days, followed by treatment with red light, and then harvested after 0, 24, and 72 h, respectively. Tuber peers were collected from the treated plantlets and immediately frozen in liquid nitrogen. To test whether red light treatment has worked or not, total glycoalkaloids and chlorophyll content of the tuber were estimated according to the previous study [5].

2.2. sRNA and Degradome Library Construction and Sequencing

Total RNA was extracted and purified from tubers using the TPK-1001 Total RNA Purification Kit (LC Science, Houston, USA) according to the manufacturer's instructions. RNA quantity and purity were analyzed using the RNA 6000 Nano LabChip Kit (Agilent, Santa Clara, CA, USA) on the Bioanalyzer 2100, with a RIN number greater than 7.0. sRNA libraries were generated following previously reported methods and were sequenced on the Illumina HiSeq 2500 at LC-BIO (Hangzhou, China). The construction of the degradome library followed a similar protocol. In brief, 20 µg of total RNA was annealed with biotinylated random primers, and RNA fragments were captured with streptavidin magnetic beads. These RNAs with 5'-monophosphates were adapter-ligated, reverse-transcribed, and PCR-amplified. The degradome cDNA libraries were sequenced on the Illumina HiSeq 2500 at LC-BIO (Hangzhou, China), as described previously (Hangzhou, China). Data generated in the study were deposited in the National Genomics Data Center (NGDC) under the accession codes of BioProject ID: PRJCA016522 and GSA submission ID: CRA010778.

2.3. Pipeline of Bioinformation Analysis

The raw reads from sRNA libraries were processed using the proprietary software package ACGT101-miR v4.2 (LC Sciences) to trim adapter dimers, junk, low complexity sequences, plant noncoding RNAs (rRNA, tRNA, snRNA, snoRNA), and repeats. Unique reads with a length between 18 and 25 nt were then aligned to species precursors in miRBase (Release 22, www.mirbase.org, accessed on 2 February 2021) [30], allowing for length variation at the 3' and 5' ends of the sequence and up to one mismatch in the alignments. Any unique read that could be mapped to potato pre-miRNAs was considered a known miRNA, while unmapped sequences were used to detect novel miRNAs. Pre-miRNA stem-loop structures were predicted using an RNAfold algorithm, with essential criteria as previously described.

To validate and classify potential targets of miRNAs, the CleaveLand4 and ACGT101-DGD-v4.0 were utilized with default parameters [31]. All sequences generated from degradome sequencing were aligned to small RNA sequences using the EMBOSS Needle program [32], and the alignments matrix was scored according to a previously described strategy for predicting plant miRNA targets. Alignments with scores not exceeding 4 and having the 5'-end of the degradome sequence coincident with the tenth nucleotide of complementarity to the small RNA were retained. Potential targets were classified into five categories using the CleaveLand4 pipeline. Gene ontology and KEGG enrichment analyses were performed using TBtools (Tbtools version 1.09876) to identify the bio-functions of miRNA-target transcripts [33].

2.4. Defining Differentially Expressed miRNAs (DEMs) and Cluster Analysis

Statistical analysis was performed using Fisher's exact test and chi-squared 2×2 test to determine the significance of miRNA expression. Light-responsive miRNAs were identified based on the combination of fold change and *p*-value. Cluster analysis and visualization of differentially expressed miRNAs (DEMs) were conducted using the Mfuzz package [34], and the number of clusters was determined by the cascadeKM function in the Vegan package [35] (R version 4.1.0).

2.5. Real-Time Quantitative Reverse Transcription Polymerase Chain Reaction (qRT-PCR) Analysis

Quantitative real-time PCR was used to quantify mRNA expression. Total RNA was reverse-transcribed, and qPCR was performed using SYBR Green Master Mix (Life Technologies, Carlsbad, CA, USA) and an ABI StepOne Plus RT-PCR system following previously established procedures [36,37]. Primer sequences used for qPCR are provided in Supplementary Table S1. The *EF1- α* and *18sRNA* gene were used as endogenous controls [38]. Fold changes in miRNA and mRNA expression were calculated using the $-\Delta\Delta C_t$ method [39]. All reactions were performed in triplicate and repeated in three independent experiments.

3. Results

3.1. Identification of Conserved miRNAs and Novel miRNAs in *S. chacoense*

Prior to high-throughput sequencing, both glycoalkaloids and chlorophyll content exhibited a gradual increase under the red-light condition (Supplemental Figure S1). Thus, it can be concluded that the experimental system was effectively functioning. To investigate the expression patterns of light-responsive miRNAs in *S. chacoense* tubers, three sRNA libraries were constructed at different light stimulus durations. The TM0h(CK), TM24h, and TM72h libraries generated 8,387,733, 14,878,292, and 9,443,424 raw reads, respectively. After filtering low-quality reads and removing known non-coding RNA families and repeat sequences, 2,508,266, 6,628,896, and 3,605,238 corresponding to 1,207,773, 3,436,592, and 1,662,556 unique reads were retained from the TM0h, TM24h, and TM72h libraries, respectively (Table 1). The size distribution patterns for both redundant and unique reads were similar across all sRNA libraries. In tuber, 24-nt and 21-nt sRNAs were the most

abundant sequences in redundant reads, with 24-nt sRNAs having the largest number of unique reads (Figure 1). These sRNA abundance and size in *S. chacoense* were consistent with other solanaceous plants, such as potato, tomato, and tobacco. Under light stimulus, the total number of 21-nt and 24-nt sRNAs was significantly higher than in darkness, indicating that light stimulus induced more sRNA loci.

Table 1. Distribution of common and specific sequences in *S. chacoense*.

Libraries	TM0h		TM24h		TM72h	
	Total	Unique	Total	Unique	Total	Unique
Raw reads	8,387,733	1,876,413	14,878,292	4,727,875	9,443,424	2,573,468
3ADT and length filter	5,430,900	631,689	6,967,261	1,187,156	4,966,215	860,198
Junk reads	15,997	13,089	58,133	46,220	26,152	19,826
Rfam	275,638	14,587	661,780	20,447	579,642	17,007
mRNA	206,800	11,482	681,823	40,578	354,377	16,525
Repeats	8383	268	14,181	353	19,755	346
rRNA	218,120	11,214	515,113	13,967	471,560	12,224
tRNA	39,211	1861	102,225	3447	75,462	2767
snoRNA	3278	214	9412	495	4807	329
snRNA	943	175	4318	660	2082	286
other Rfam RNA	14,086	1123	30,712	1878	25,731	1401
valid reads	2,508,266	1,207,773	6,628,896	3,436,592	3,605,238	1,662,556

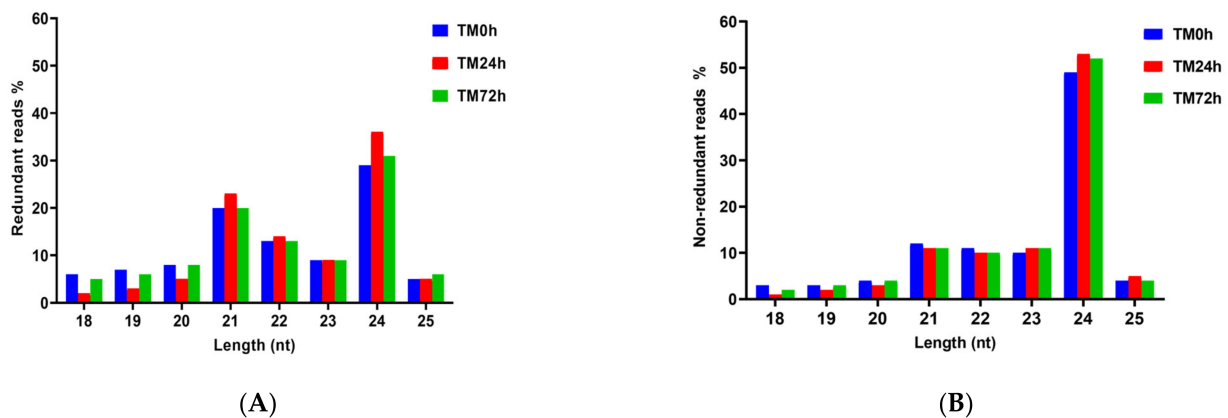


Figure 1. (A) The length distribution of redundant reads in small RNA libraries. (B) The length distribution of non-redundant reads in small RNA libraries. The samples treated with continuous light at 24h and 72h were called TM24h and TM72h, respectively.

To identify known and novel miRNAs in the three libraries, the remaining sequences were aligned to potato miRNA precursors (pre-miRNAs) or mature miRNA sequences in miRbase v22.0. A total of 732 unique miRNAs corresponding to 676 pre-miRNAs were identified in *S. chacoense* (Table 2 and Supplementary Table S2). MiRNAs in Group 1a were potato-specific, while those in group 1b, group 2, and group 3 were conservative miRNAs (Table 2 and Supplementary Table S2). Most identified miRNAs were highly homologous to other plant species, such as *Solanum tuberosum*, *Glycine max*, *Populus trichocarpa*, *Malus domestica*, *Oryza sativa*, and *Zea mays*. All identified miRNAs belonged to 59 miRNA families, with conserved miRNA families playing an important role in stress responses in various plant species. Among these families, 12 highly conserved miRNA families were identified, with miR156 being the largest conserved family, having 32 members (Supplementary Table S3). Additionally, 179 novel miRNAs (group 4) corresponding to 174 bona fide precursors were identified in *S. chacoense* (Table 2 and Supplementary Table S2). These novel miRNA precursors ranged from 60 to 219 nt in length, with MFEI values ranging from 0.9 to 2.4. A total of 145 novel miRNAs were mapped to a single locus, while 34 novel miRNAs were mapped to multiple locations in the potato genome (Supplementary Table S2). Interestingly, 83 novel miRNAs were expressed at middle levels, and one novel miRNA was expressed at high levels in *S. chacoense* (Supplementary Table S2). Predicted miRNAs showed uridine (U)

and adenine (A) bias at the 5' end, with the first position predominantly occupied by U and A (Figure 2A). Additionally, the 10th nucleotides were predominantly U and A in all predicted miRNAs and novel miRNAs (Figure 2B).

Table 2. Summary of known and predicted miRNAs in *S. chacoense*.

Category *	Total Pre-miRNA	Total Unique miRNA	TM0h Pre-miRNA	TM0h Unique miRNA	TM24h Pre-miRNA	TM24h Unique miRNA	TM72h Pre-miRNA	TM72h Unique miRNA
Group 1a	141	198	113	136	141	197	111	147
Group1b	39	60	30	46	39	60	34	51
Group2a	61	70	54	59	61	70	50	57
Group2b	213	177	174	134	213	176	186	149
Group3	48	48	30	30	47	47	32	32
Group4	174	179	119	112	173	178	125	117

* gp1a: Reads map to potato miRNAs/pre-miRNAs in miRbase and the pre-miRNAs further map to the potato genome. gp1b: Reads map to selected (except for specific) miRNAs/pre-miRNAs in miRbase and the pre-miRNAs further map to the potato genome. gp2a: Reads map to potato miRNAs/pre-miRNAs in miRbase. The mapped pre-miRNAs do not map to the genome, but the reads (and of course the miRNAs of the pre-miRNAs) map to potato genome. The extended genome sequences from the genome loci may form hairpins. gp2b: Reads were mapped to miRNAs/pre-miRNAs of selected species (except for specific) in miRbase and the mapped pre-miRNAs were not further mapped to potato genome, but the reads (and of course the miRNAs of the pre-miRNAs) were mapped to potato genome. The extended genome sequences from the genome loci may not form hairpins. gp3: Reads map to selected miRNAs/pre-miRNAs in miRbase. The mapped pre-miRNAs do not map to the potato genome, and the reads do not map to the potato genome. gp4: Reads do not map to selected pre-miRNAs in miRbase. But the reads map to potato genome and the extended genome sequences from genome may form hairpins.

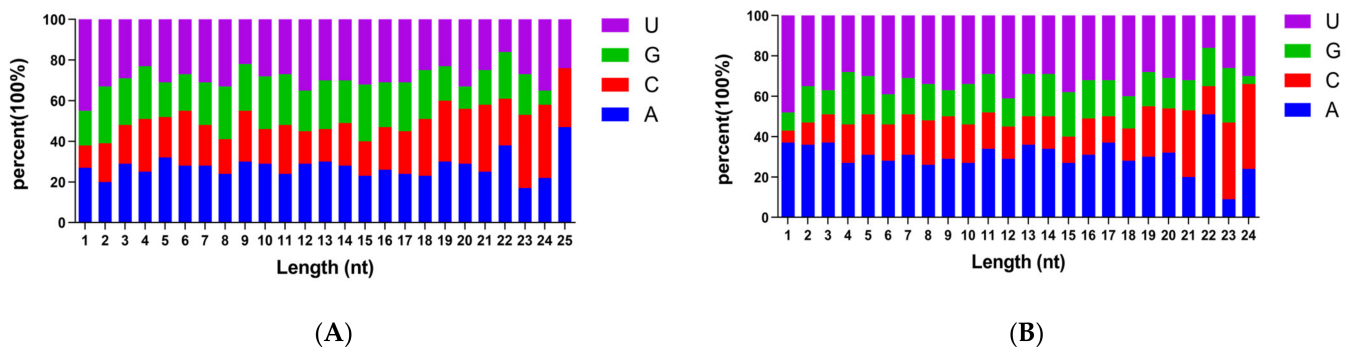


Figure 2. (A) Relative nucleotide bias of all predicted miRNAs. (B) Relative nucleotide bias of novel miRNAs.

3.2. Target Prediction and Identification via *In Silico* and Degradome Approaches

In total, we obtained 20,749,711, 20,114,323, and 19,663,065 raw reads from TD0h, TD24h, and TD72h libraries, respectively (Table 3). After removing the 3' adapter, a total of 7,961,145, 7,939,131, and 7,482,735 unique reads were aligned to the potato genome (Table 3). Of these, 4,316,514 (12,438,537), 4,241,085 (11,769,904), and 4,107,240 (11,982,016) unique reads were found to align well with annotated potato transcripts. The mapped reads from the TD0h, TD24h, and TD72h libraries represented 36,626 (81.66%), 36,894 (82.26%), and 36,462 (81.30%) annotated potato transcripts, respectively (Table 3). The majority of annotated potato transcripts had at least one matched tag among the three libraries.

Table 3. Summary of degradome sequencing in *S. chacoense*.

Sample	TD0h (Number)	TD24h (Number)	TD72h (Number)
Raw Reads	20,749,711	20,114,323	19,663,065
Unique Raw Reads	7,961,145	7,939,131	7,482,735
Reads < 15 nt after removing 3' adaptor	160,233	151,083	148,593
Mappable Reads	20,589,478	19,963,240	19,514,472
Unique reads < 15nt after removing 3' adaptor	62,376	60,612	58,916
Unique Mappable Reads	7,898,769	7,878,519	7,423,819
Mapped Reads	12,438,537	11,769,904	11,982,016
Unique Mapped Reads	4,316,514	4,241,085	4,107,240
Number of input Transcript	44,851	44,851	44,851
Number of Covered Transcript	36,626	36,894	36,462

We applied the Cleveland program to identify cleaved targets for known miRNAs and novel miRNAs, dividing the cleaved transcripts into five degradome categories based on the relative abundance of the cleavage tags at the target transcript sites. We identified a total of 6335 unique target transcripts that could be cleaved by 489 known and 153 novel miRNAs in the three libraries. Among these identified targets, 3565, 3682, and 3406 target transcripts were identified in the TD0h, TD24h, and TD72h libraries, respectively. A Venn diagram showed that 1380 transcripts were common among the three degradome libraries, and 1195 transcripts were identified only in the TD0h degradome library (Figure 3). Under light stimulus, a total of 1182 and 1020 transcripts were identified in the TD24h and TD72h degradome libraries, respectively (Figure 3), indicating that miRNA-mediated target cleavage was stimulated by continuous light.

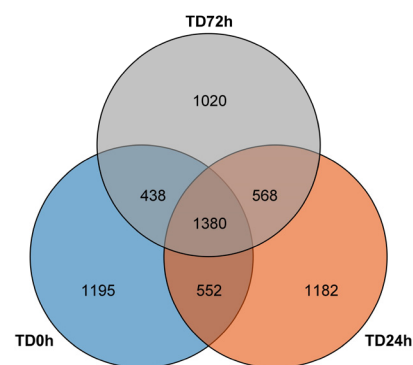


Figure 3. Venn diagrams represent genome-matched transcripts of specific transcripts and common transcripts among TD0h, TD24h and TD72h libraries. The control sample treated with darkness condition was called TD0h. The samples treated with continuous light at 24 h and 72 h were called TD24h and TD72h, respectively.

To depict the biological function of target transcripts cleaved by miRNAs, we performed gene ontology (GO) classification to assign GO terms. Under light stimulus, more GO terms were found to be enriched in the TD24h and TD72h libraries. GO enrichment revealed that transcripts in the TD24h libraries were significantly enriched in 'cell', 'cytosolic small ribosomal subunit', 'RNA secondary structure unwinding', 'unfolded protein binding', 'ATP-dependent RNA helicase activity', 'thylakoid', 'mRNA binding', 'protein folding', and other related terms (Figure 4A). Additionally, GO enrichment analysis showed that GO terms related to 'ATP synthesis coupled proton transport', 'response to high light intensity', 'unfolded protein binding', 'RNA splicing', 'glycolytic process', 'cytosolic small ribosomal', and 'mRNA binding' were enriched in the TD72h library (Figure 4B).

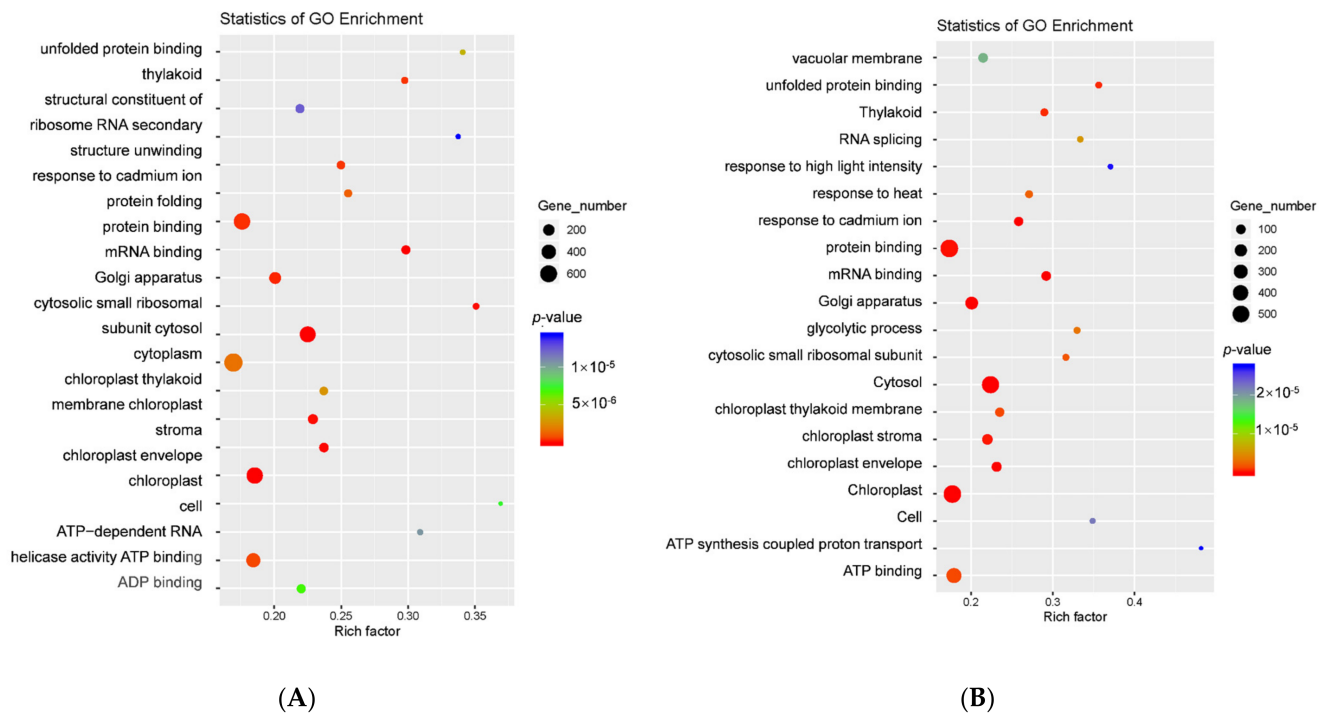


Figure 4. (A) The top 20 GO terms of differentially expressed transcripts mediated by miRNAs under 24 h of light. (B) The top 20 GO terms of differentially expressed transcripts mediated by miRNAs under light stimulus under 72 h of light. Rich factor indicates the ratio of differentially expressed transcripts enriched in the GO terms among genes annotated in the GO term.

We also performed KEGG pathway analysis, classifying 2065 target transcripts into 135 pathways. KEGG enrichment analysis revealed that transcripts in the TD24h library were significantly enriched in ‘synthesis and degradation of ketone bodies’, ‘glycosphingolipid biosynthesis’, ‘carbon fixation in photosynthetic organisms’, ‘TCA cycle’, ‘mRNA surveillance pathway’, ‘Phenylalanine, tyrosine and tryptophan biosynthesis’, ‘Porphyrin and chlorophyll metabolism’, ‘Pyruvate metabolism’, and other related pathways (Figure 5A). In the TD72h library, the transcripts’ target enrichment analysis revealed significant KEGG pathways, including ‘taurine and hypotaurine metabolism’, ‘TCA cycle’, ‘pyruvate metabolism’, ‘Spliceosome’, ‘photosynthesis-antenna proteins’, ‘Phenylalanine, tyrosine and tryptophan biosynthesis’, and ‘mRNA surveillance pathway’ (Figure 5B).

3.3. Identification and Cluster Visualization of Light-Responsive miRNAs

To identify light-responsive miRNAs and determine the expression patterns of differentially expressed miRNAs (DEMs) in response to light, we compared the abundances of miRNA reads among three small RNA (sRNA) libraries. Statistical analyses revealed that 154 miRNAs were differentially expressed between TM24h and TM0h libraries, with 113 up-regulated and 41 down-regulated by light stimulus (Figure 6A). Similarly, we analyzed the expression profiling of miRNAs between TM72h and TM0h libraries, and a total of 105 miRNAs were up-regulated and 110 were down-regulated after 72 h of exposure to light (Figure 6A). Moreover, a total of 210 DEMs were detected between TM72h and TM24h libraries, with 67 upregulated and 143 downregulated by light stimulus. These results indicate a significant change in the number of DEMs after light exposure. A Venn diagram of DEMs among the different samples showed that 11 DEMs were common in all three libraries (Figure 6B).



Figure 5. (A) The top 20 KEGG pathways of differentially expressed transcripts mediated by miRNAs under 24 h of light. (B) The top 20 KEGG pathways of differentially expressed transcripts mediated by miRNAs under light stimulus under 72 h of light. Rich factor indicates the ratio of differentially expressed transcripts enriched in the pathway among genes annotated in the pathway.

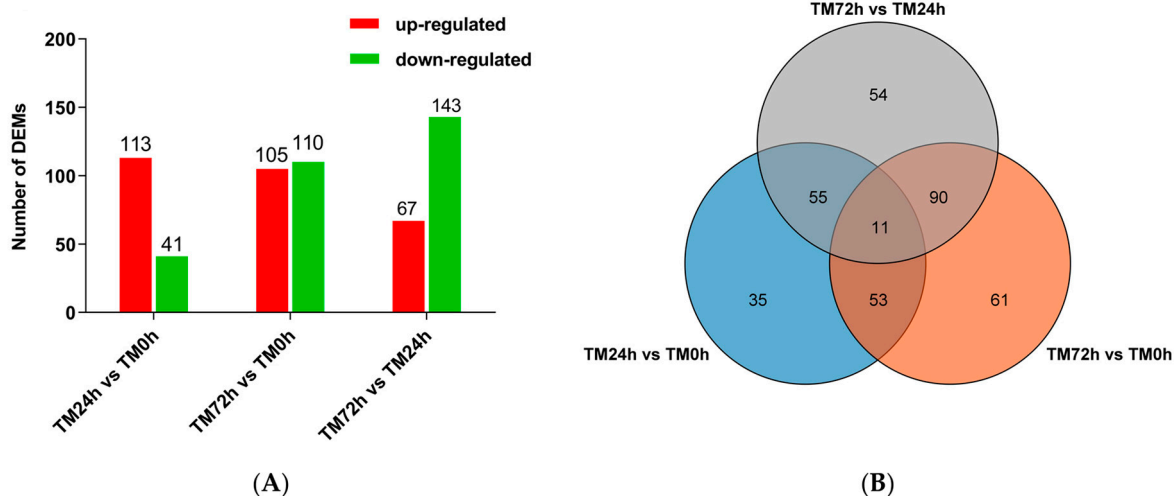


Figure 6. (A) The number of miRNAs up- or down-regulated in response to light at 24 h and 72 h. (B) Distribution of DEMs among TM0h, TM24h and TM72h libraries.

To further clarify the expression patterns of DEMs, a k-mean cluster analysis was performed using the Mfuzz package. The DEMs were categorized into eight temporally related clusters (Figure 7A), with three up-regulated groups (k2, k5, k7) and three down-regulated groups (k1, k4, k8) based on their dynamic expression patterns. The up-regulated and down-regulated groups contain 139 and 167 miRNAs, respectively. In addition, the expression of DEMs in cluster k6 showed a peak of expression at 24 h of light exposure, while cluster k3 DEMs showed higher expression levels in darkness conditions and dramatically decreased at 24 h of light exposure. The results of the k-means cluster indicate that specific miRNAs can be dynamically regulated by light, suggesting that these miRNAs may be involved in various biological processes. To validate the results from degradome sequencing, a total of 12 differentially expressed miRNAs and targets were verified by qRT-PCR under different conditions (0 h, 24 h, and 72 h of light stimulus). The results show

a consistent expression trend between degradome sequencing and qRT-PCR (Figure 8 and Supplemental Figure S2). Interestingly, six target transcripts showed approximately inverse expression patterns with their corresponding miRNAs. For example, ath-MIR8175-p3 was down-regulated at 24 h and 72 h of light stimulus, while the ath-MIR8175-p3 targeted *AKIN beta2* gene was up-regulated at 24 h and 72 h of light stimulus. The inverse expression patterns were also observed in nta-miR172j/*APETALA2*, mdm-miR408a/*PPR*, nta-miR156a/*SPL*, PC-5p-33341_35/*CIPK*, and stu-miR482c/*3-BETA HYDROXYSTEROID DEHYDROGENASE* (Figure 8).

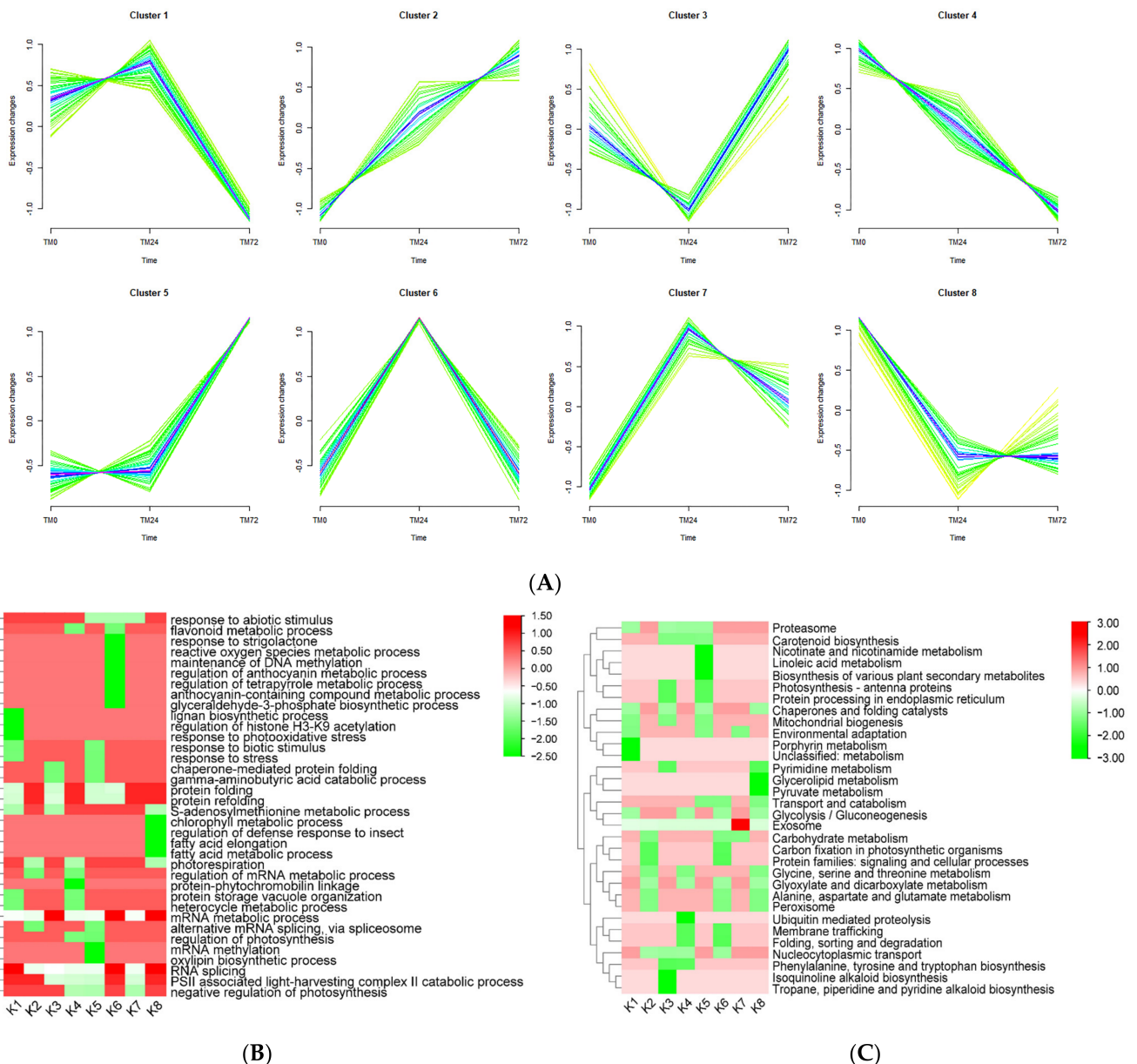


Figure 7. (A) Cluster visualization of light-responsive miRNAs. Green, yellow, blue or purple colored lines correspond to miRNAs with different membership value. (B) GO enrichment analysis of transcripts regulated by eight light-responsive miRNA clusters. (C) KEGG pathway enrichment analysis of transcripts regulated by eight light-responsive miRNA clusters. The green and red color indicate the *p*-value of significantly enriched GO terms/KEGG pathways.

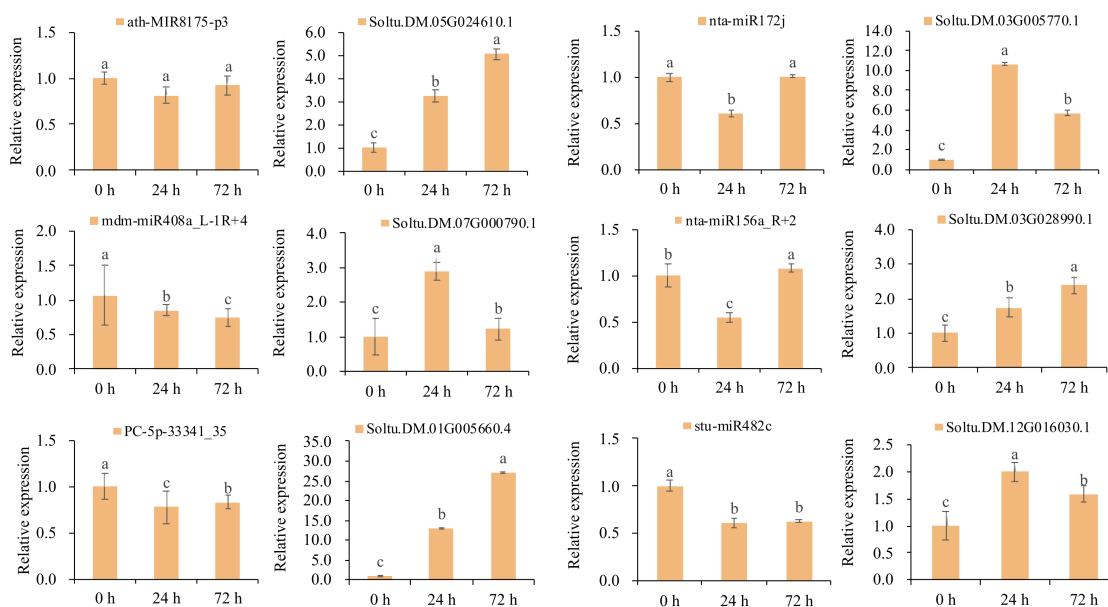


Figure 8. Validation of degradome sequencing result by qRT-PCR (*EF1- α* gene was used as control). All qRT-PCR results are represented as mean values \pm SD. Letters (a–c) indicate significant differences ($p < 0.05$).

3.4. Function Annotation of Regulatory Networks Mediated by miRNAs Responsive to Light

We have identified light-responsive miRNAs in *S. chacoense* and determined the functions of miRNA-based regulatory networks. Using degradome sequencing results, we constructed miRNA regulatory networks comprising miRNA-target pairs in eight temporally related miRNA clusters. Subsequently, we performed GO and KEGG enrichment analyses for miRNA target-pairs in these eight clusters. The target transcripts in the eight clusters were associated with a broad spectrum of biological processes, indicating that miRNAs play a crucial role in various physiological processes. In the up-regulated clusters (k2, k5, k7), the miRNA targets appeared to be involved in various biological processes, including ‘mRNA metabolic process’, ‘RNA splicing’, ‘photorespiration’, ‘regulation of mRNA metabolic process’, ‘protein folding’, ‘negative regulation of photosynthesis’, ‘response to abiotic stimulus’, ‘response to stress’, ‘mRNA methylation’, and ‘oxylipin biosynthetic process’ (Figure 7B). Conversely, in the down-regulated clusters (k1, k4, k8), miRNAs appeared to be involved in biological processes such as ‘protein storage vacuole organization’, ‘heterocycle metabolic process’, ‘S-adenosylmethionine metabolic process’, ‘protein folding’, ‘response to photooxidative stress’, ‘regulation of histone H3-H9’, ‘lignan biosynthetic process’, ‘flavonoid metabolic process’, ‘RNA splicing’, ‘fatty acid elongation’, ‘regulation of defense response to insect’, and ‘chlorophyll metabolic process’ (Figure 7B). In cluster k3, GOBP terms were over-represented in ‘RNA splicing’, ‘S-adenosylmethionine metabolic process’, ‘chaperone-mediated protein folding’, and ‘GABA catabolic process’. Additionally, cluster k7 was enriched with ‘PSII associated light-harvesting complex II catabolic process’, ‘negative regulation of photosynthesis’, ‘RNA splicing’, and ‘response to abiotic stimulus’ (Figure 7B).

Enriched KEGG analysis revealed that miRNA targets in up-regulated clusters (k2, k5, k7) were associated with ‘carbohydrate’, ‘carbon fixation in photosynthetic organisms’, ‘protein families: signaling and cellular processes’, ‘glycine, serine and threonine metabolism’, ‘glyoxylate and dicarboxylate metabolism’, ‘alanine, aspartate and glutamate metabolism’, ‘peroxisome’, ‘exosome’, ‘carotenoid biosynthesis’, ‘transport and catabolism’, ‘chaperones and folding catalysts’, ‘proteasome’, ‘biosynthesis of various plant secondary metabolism’, ‘linoleic acid metabolism’, ‘nicotinate and nicotinamide metabolism’, ‘protein processing in endoplasmic reticulum’, and ‘environmental adaptation’ (Figure 7C). Conversely, down-regulated clusters (k1, k4, k8) were associated with miRNAs involved in pathways such

as ‘glycolysis’, ‘chaperones and folding catalysts’, ‘proteasome’, ‘porphyrin metabolism’, ‘ubiquitin mediated proteolysis’, ‘membrane trafficking’, ‘folding, sorting and degradation’, ‘nucleocytoplasmic transport’, ‘phenylalanine, tyrosine, and tryptophan biosynthesis’, ‘carotenoid biosynthesis’, ‘glycine, serine and threonine metabolism’, ‘glyoxylate and dicarboxylate metabolism’, ‘pyrimidine metabolism’, ‘glycerolipid metabolism’, ‘pyruvate metabolism’, and ‘alanine, aspartate and glutamate metabolism’ (Figure 7C). In cluster k3, KEGG pathways were enriched in ‘isoquinoline alkaloid biosynthesis’, ‘tropane, piperidine and pyridine alkaloid biosynthesis’, ‘phenylalanine, tyrosine, and tryptophan biosynthesis’, ‘carotenoid biosynthesis’, and ‘pyrimidine metabolism’. Additionally, ‘carbohydrate metabolism’ and ‘environmental adaptation’ were enriched in cluster k7 (Figure 7C). Taken together, these enriched GO terms and KEGG pathways provide valuable insights into the roles of miRNAs in response to light in *S. chacoense*.

3.5. Subnetworks Analysis Identifies Important Functional miRNA-Target Interactions

In general, the target transcripts of the nine miRNA clusters identified in this study are mainly transcription factors involved in stress responses, metabolic pathways, and steroidal glycoalkaloid biosynthesis. For instance, in cluster k1 (Supplementary Table S4), ath-miR396b-5p_1ss21TA targeted *GROWTH-REGULATING FACTORS*, nta-miR172c_L-1R + 1 targeted *ETHYLENE-RESPONSIVE TRANSCRIPTION FACTORS*, and stu-miR156a targeted *SBP* transcription factors. Moreover, sly-miR482d-5p_R-3 and PC-3p-48732_21 targeted *MYB* and *NAC* transcription factors, respectively. Some miRNAs also target transcripts related to metabolic pathways. For example, sly-miR396a-5p targeted two *CYTOCHROME P450 71A9-LIKE*, while sly-miR482d-5p_R-3 targeted *CYTOCHROME P450 83B1-LIKE* and *CYTOCHROME P450 89A2-LIKE*. In cluster k8 (Supplementary Table S4), down-regulated miRNAs targeted *AP2/ERF*, *SBP*, *bHLH*, and *WRKY* transcription factors. Furthermore, *DIHYDROFLAVONOL-4-REDUCTASE-LIKE PROTEIN* targeted by osa-MIR2118e-p3_2ss13TA19CT may be associated with flavonoid biosynthesis. In cluster k4 (Supplementary Table S4), several miRNAs targeted *WRKY*, *MYB*, *GAMYB*, and *AP2/ERF* transcription factors. Two light-responsive miRNAs (stu-MIR156a-p3 and nta-miR397_L + 2R-3) were found to target *ALDEHYDE OXIDASE AND PHYTOENE SYNTHASE 1*, indicating their potential role in carotenoid biosynthesis. Additionally, stu-MIR156a-p3 targeted *CYTOCHROME P450 86A8-LIKE*, which is involved in the cutin, suberine, and wax biosynthesis pathways. Six miRNAs (PC-5p-160931_4, gma-miR399d_R-1_1ss13TA, nta-miR172j_1ss1GT, nta-miR397_L + 2R-3, stu-MIR156c-p3, and stu-miR399i-3p) were found to target transcripts involved in the ubiquitin-mediated proteolytic pathway. Finally, gma-miR6300_1ss3CG may function as a key controller in terpenoid backbone biosynthesis by cleaving *ISOPENTENYL-DIPHOSPHATE DELTA-ISOMERASE I-LIKE* and *ISOPENTENYL-DIPHOSPHATE DELTA-ISOMERASE I* transcripts.

In cluster k2 (Supplementary Table S4), PC-5p-6788_133 targeted transcripts related to linoleic acid metabolism and steroid biosynthesis. Furthermore, several miRNA-target pairs were identified, regulating transcription factors such as osa-miR156b-3p_5ss8CT9TC10CT11 TC14-T and *BHLH62 TRANSCRIPTION FACTOR*, sly-miR166a_L + 2R-2_2 and *BHLH112-LIKE TRANSCRIPTION FACTOR*, stu-miR156f-3p_L-1 and *SBP TRANSCRIPTION FACTORS*, among others. In cluster k5 (Supplementary Table S4), five miRNA-target pairs appear to regulate steroid biosynthesis, including osa-MIR6255-p3_2ss10TC18GT and *STEROL 14-DEMETHYLASE*, ptc-miR6478_2ss7TA21GA and *DELTA(24)-STEROL REDUCTASE-LIKE ISOFORM X1*, sly-miR319c-5p_1ss13AG and *DELTA(24)-STEROL REDUCTASE-LIKE ISOFORM X1*, and stu-MIR5303j-p5_2ss10GT17CT and *METHYLSTEROL MONOOXYGENASE 1-1-LIKE* and *CYCLOARTENOL-C-24-METHYLTRANSFERASE-LIKE*. In addition, two miRNA-target pairs might participate in cutin, suberine, and wax biosynthesis, including ath-MIR8175-p3_2ss14TC18AC_1 and *RHODANESE-LIKE DOMAIN-CONTAINING PROTEIN 9*, osa-MIR6255-p3_2ss10TC18GT and *FATTY ACYL-COA REDUCTASE 3*. Additionally, ppe-miR858_R-3_1ss4GA targets five transcripts related to linoleic acid metabolism. In cluster k7 (Supplementary Table S4), gma-miR399i_R-1_1ss7AG and sly-MIR167b-p3

may play an important role in glutathione metabolism by cleaving *GLUTATHIONE S-TRANSFERASE T1-LIKE*, *5-OXOPROLINASE*, *ASCORBATE PEROXIDASE*, and *L-ASCORBATE PEROXIDASE*, respectively. Moreover, under light stimulus, four universal stress protein transcripts are the target of sly-MIR167b-p3. In cluster k3 (Supplementary Table S4), sly-miR164b-3p targets four *CBL-INTERACTING SERINE/THREONINE-PROTEIN KINASES (CIPKs)*. Additionally, *CIPK* is a critical component of the CBL-CIPK signaling pathway and participates in regulating various biological processes [40]. Identification of the *CIPK* gene indicated that sly-miR164b-3p might be involved in the CBL-CIPK signaling pathway by regulating the expression of *CIPK* transcripts. Furthermore, sly-miR164b-3p and stu-miR827-5p are associated with steroid biosynthesis by targeting *CYCLOARTENOL-C-24-METHYLTRANSFERASE* and *STEROL 14-DEMETHYLASE*, respectively. In cluster k6 (Supplementary Table S4), stu-miR8026_L-2R-1_1ss17GA and PC-5p-104288_7 target three distinct transcripts related to the terpenoid backbone biosynthesis pathway. Moreover, stu-miR482e-5p targets a *DELTA(7)-STEROL-C5(6)-DESATURASE-LIKE transcript* associated with steroid biosynthesis.

4. Discussion

4.1. Identification of Conserved miRNAs and miRNA Candidates in *S. chacoense*

In recent years, genome-wide approaches have been utilized to identify plant miRNAs that respond to stress in a temporal-specific manner. The resulting findings suggest that miRNA profiles not only play critical roles in abiotic stress responses, but also have profound effects on cell metabolism and physiological traits during such stress. In this study, we identified 16 highly evolutionarily conserved miRNA families in *S. chacoense*, which are also present in cultivated potato. Notably, the conserved miRNAs in *S. chacoense* exhibited much higher expression levels than the non-conserved miRNAs. A genome-wide investigation revealed that the pre-miRNAs of these conserved miRNAs are present at multiple loci in *S. chacoense*, and are expressed abundantly. Previous research has shown that such conserved miRNAs with multiple loci may arise from large-scale genomic duplications and rearrangements in the plant genome. Among these conserved miRNA families, some contain diverse canonical variants (isomiRs) in solanaceous plants (e.g., miR156, miR166, miR171, miR172, miR319, and miR399), while others contain only a few isomiRs (e.g., miR394, miR476, miR535, miR8041, and miR8038). Previous research has revealed that isomiRs play a critical role in the regulation of various abiotic and biotic responses [41,42]. In addition, we found many isomiRs that were significantly differentially expressed in the tubers of *S. chacoense* under light stimulus. Although these isomiRs can be categorized into miRNA families, the identification of stress-responsive isomiRs and their differential targets suggests that isomiRs may play important roles in fluctuating environmental conditions.

4.2. Differentially Expressed miRNAs Involved in Abiotic Stress Response

In this study, we identified both known and novel miRNAs that were differentially regulated by light stimulus in *S. chacoense*. We employed a K-means clustering approach to categorize the differentially expressed miRNAs into nine temporal clusters. These light-responsive miRNAs displayed four distinct expression patterns, including consistently upregulated, consistently downregulated, early upregulated, and early downregulated miRNAs. Studies in *Solanum tuberosum* L. [10], *B. rapa* [43], and *A. thaliana* [44] have demonstrated that miRNAs are differentially regulated by light, thereby advancing our understanding of miRNA regulation in response to light stimuli. For instance, previous research in potato showed that eight isomiRs of miRNA families (miR166, miR397, miR399, miR477, miR482, miR7994, miR8032, and miR8036) were upregulated in tuber under light stimulus, while seven isomiRs of miRNA families (miR399, miR479, miR6023, miR6024, miR6027, miR8020, and miR8023) were downregulated [10]. Similarly, in *B. rapa*, eight miRNA families (miR391, miR1439, miR2111, miR2911, miR2916, miR3630, miR5083, and miR5175) were upregulated, whereas four miRNA families (miR396, miR1535, miR1885, miR5138) were downregulated under UV-A light [43]. In *A. thaliana* [44], 11 miRNA families

(miR156, miR159, miR160, miR165, miR167, miR169, miR170, miR172, miR393, miR398, and miR401) were upregulated under UV-B light. In our research, we found that some of the previously identified light-responsive miRNAs in cultivated potato were consistently up- or down-regulated under light illumination. For instance, isomiRs of miR156, miR166, miR168, miR396, and miR408 were upregulated under light stimulus, while isomiRs of miR399 and miR6023 were downregulated, which is consistent with previous studies in *A. thaliana* or cultivated potato. Collectively, these light-responsive miRNAs in different plant species displayed similar expression trends under various spectrums of light, suggesting that the promoter of these miRNA genes may harbor some light-relevant cis-elements.

Cross-tolerance is a phenomenon in which exposure to one type of stress can induce tolerance to several other types of stress. Transcription factors, reactive oxygen species (ROS), heat shock proteins (HSPs), and small RNAs are key components in the crosstalk across different stress-related pathways [45,46]. In our study, a set of light-responsive miRNAs has been shown to be associated with abiotic and biotic stresses. For example, ath-miR858b_2ss1TC4GA in cluster k5 targets a MYB transcription factor that encodes a protein with high homology to MYB59 in *A. thaliana*, which can be induced by cadmium (Ca) or cyst nematode attack [47]. The identification of this MYB factor suggests that ath-miR858b_2ss1TC4GA may participate in multiple stresses by regulating the abundance of MYB transcripts. Additionally, stu-MIR530-p3_1ss9GA in cluster k5 targets five transcripts of HSPs that are involved in protein processing in the endoplasmic reticulum pathway. HSPs can be induced by cold, drought, heat flooding, and oxidative stress, and they play a crucial role in protecting plants from various abiotic stresses [48,49]. Furthermore, a transcript targeted by ptc-miR6478_2ss7TA21GA in cluster k5 exhibits significant similarity to EIN3-BINDING F BOX PROTEIN (EBF1/EBF2) in *A. thaliana*. Previous studies have reported that ethylene and salt stress reduce EBF1/EBF2 protein levels, leading to an accumulation of EIN3/EIL1 and increased peroxidase (POD) activity [50]. The identification of this EBF1/EBF2 gene under light stimulus suggests that upregulated ptc-miR6478_2ss7TA21GA may participate in ROS regulation by regulating the expression of EIN3-BINDING F BOX gene. In conclusion, these findings demonstrate that light-responsive miRNAs can modulate transcript abundance of MYB59, HSPs, and EBF1/EBF2, thereby contributing to cross-tolerance responses to abiotic and biotic stresses.

4.3. miRNAs and Target Transcripts Are Important for Primary and Secondary Metabolism

Interestingly, many light-responsive miRNAs and target transcripts are associated with primary and secondary metabolic pathways. Recently, a NADPH-dependent enzyme related to flavonoid biosynthesis in *A. thaliana* [51] or *Brassica napus* L. [52], DIHYDROFLAVO NOL-4-REDUCTASE, was identified. In this study, we found that osa-MIR2118e-p3_2ss13TA19CT targets DIHYDROFLAVONOL-4-REDUCTASE, indicating that the miRNA can regulate flavonoid biosynthesis pathways in potato plants. Additionally, isomiRs of miR11471 (pab-MIR11471-p3_2ss1CA18TG) target a transcript with high similarity to a bHLH transcription factor (BHLH121) in *A. thaliana*, which plays an important role in iron homeostasis and may indirectly regulate downstream genes involved in specific metabolic processes [53,54]. Recently, Koichi reported that GLUTAMATE-1-SEMIALDEHYDE 2,1-AMINOMUTASE (GSA aminotransferase, GSAT) and GERANYL-GERANYL REDUCTASE (CHLP) are important genes involved in tetrapyrrole biosynthesis in *A. thaliana* [11]. In our degradome sequencing libraries, we identified homology genes of GSAT and CHLP targeted by ppe-miR858_R-3_1ss4GA and ath-miR8175_1ss12AG (osa-miR5072_L-3) in the light stimulus, respectively. Thus, the identification of GSAT and CHLP in this study revealed that two light-responsive miRNAs have important roles in post-transcriptional regulation of tetrapyrrole biosynthesis.

Furthermore, the CYP86A33 gene has been reported to have a novel function in suberin biosynthesis, conferring resistance to potato tuber greening [20]. Accordingly, we have identified a CYP86A33 transcript targeted by sly-MIR172b-p5, which was highly expressed in potato tuber response to light, implying miR172 isomiRs may have an important role in

suberin biosynthesis. We also found several *SPL* transcription factors (*SPL1*, *SPL3*, *SPL6*, *SPL9*, *SPL12*, and *SPL16*) targeted by isomiRs of miR156 in the consistently downregulated cluster (k1, k4, and k8). In *A. thaliana* and *Pogostemon cabin*, miR156-targeted *SPLs* regulate the expression of *TPS* gene family, which is involved in sesquiterpenes biosynthesis [55]. Hence, the miR156-*SPLs* module may have an indirect molecular link with steroidal glycoalkaloid biosynthesis because the metabolites derived from sesquiterpenes precursors are considered to be the origin of steroidal glycoalkaloid biosynthesis [56].

Moreover, several light-responsive miRNAs were identified to cleave target transcripts related to steroidal glycoalkaloid/steroid biosynthesis by degradome sequencing (Supplementary Table S5). For instance, isomiRs of ath-MIR5017/ath-MIR8175 family can cleave target transcripts *SNF1-RELATED PROTEIN KINASE* in cluster k5 (Supplementary Table S5). Previous studies reported that *SNF1-RELATED PROTEIN KINASE* (AT3G01090 and AT3G29160) [57] can inhibit isoprenoid synthesis by phosphorylation of *HMG-CoA REDUCTASE* [58]. *HMG-CoA REDUCTASE* is a key enzyme in the mevalonate/isoprenoid pathway, and glycoalkaloids are products of isoprenoid in potatoes [59]. The identification of *SNF1-RELATED PROTEIN KINASE* demonstrates that ath-MIR5017/ath-MIR8175 may regulate steroidal glycoalkaloid biosynthesis by phosphorylating *HMG-COA REDUCTASE*. Additionally, a novel miRNA, pab-MIR11471-p5_2ss17TG18 CG (Supplementary Table S5), targets *CYTOCHROME P450* (PGSC0003DMG400011750), which is tightly co-expressed with genes associated with steroidal alkaloids in solanaceous crops [8]. Seven MTIs regulating the steroid biosynthesis pathway were identified (Supplementary Table S5), including stu-MIR5303j-p5_2ss10GT17CT/*CYCLOARTENOL-C-24-METHYLTRANSFERASE*, stu-miR827-5p/*STE-ROL 14-DEMETHYLASE*, and sly-miR319c-5p_1ss13AG/*DELTA (24)-STEROL REDUCTASE* modules. These MTIs are responsible for regulating the isoprenoid biosynthesis, terpenoid biosynthesis and steroid biosynthesis pathway. Furthermore, these miRNAs may regulate diversity, biological activities, and biosynthesis of steroidal glycoalkaloids through the SGA biosynthesis pathways.

5. Conclusions

Taken together, our data not only provide a valuable resource for identifying light-responsive miRNAs in potatoes, but also suggest the MTIs governing secondary metabolic pathways. An integrative miRNA-mediated gene interaction network was uncovered, containing miRNA-mRNA target pairs related to isoprenoid biosynthesis, terpenoid biosynthesis and steroid biosynthesis pathways. The mechanism of interaction among the genes in the MTIs needs to be further studied, but the results offer a comprehensive understanding of the molecular mechanism behind sterol and steroid biosynthesis. Likewise, we propose a novel strategy for precise manipulation of metabolic pathways, aimed at reducing potato toxicity through epigenetic means.

Supplementary Materials: The following supporting information can be downloaded at: <https://www.mdpi.com/article/10.3390/agronomy13071763/s1>, Table S1: Oligonucleotide primers used in real-time PCR; Table S2: Summary of known and predicted miRNA in *S. chacoense*; Table S3: Summary of all miRNA families in *S. chacoense*; Table S4: Target transcripts mediated by differentially expressed miRNAs; Table S5: Light-responsive MTIs related to putative SGA pathway in *S. chacoense*; Figure S1: The total glycoalkaloids and chlorophyll content of *S. chacoense* treated with red light for 0 (CK), 24 and 72 h; Figure S2: Validation of degradome sequencing result by qRT-PCR (*18sRNA* gene was used as control).

Author Contributions: Conceptualization, Y.Q.; methodology, Q.L.; software, P.A.; validation, P.R. and D.L.; formal analysis, P.R. and F.Y.; investigation, D.L.; resources, F.Y.; data curation, J.X.; writing—original draft preparation, Y.Q.; writing—review and editing, Y.Q. and P.A.; visualization, P.R.; supervision, Y.Q.; project administration, Q.L.; funding acquisition, Y.Q. All authors have read and agreed to the published version of the manuscript.

Funding: This work is supported by the National Natural Science Foundation of China (Grant No. 31960441). This work is supported in part by the National Natural Science Foundation of Gansu

Province, China (Program No.18JR3RM236), the National Natural Science Foundation of Qinyang City, China (Program No. QY-STK-2022A-006). This work is also supported by the Longdong University Doctoral Scientific Research Foundation (XYBY1706).

Data Availability Statement: The raw sequence data reported in this paper have been deposited in the Genome Sequence Archive (Genomics, Proteomics & Bioinformatics 2021) in National Genomics Data Center (Nucleic Acids Res 2022), China National Center for Bioinformation/Beijing Institute of Genomics, Chinese Academy of Sciences (GSA: CRA010778) that are publicly accessible at <https://ngdc.cncb.ac.cn/gsa>, accessed on 25 April 2023.

Acknowledgments: We appreciate that all the authors contribute to this manuscript and thank all anonymous reviewers for their constructive advice.

Conflicts of Interest: The authors declare no conflict of interest.

References

1. Devaux, A.; Goffart, J.P.; Kromann, P.; Andrade-Piedra, J.; Polar, V.; Hareau, G. The potato of the future: Opportunities and challenges in sustainable agri-food systems. *Potato Res.* **2021**, *64*, 681–720. [[CrossRef](#)] [[PubMed](#)]
2. Naeem, M.; Tetlow, I.; Emes, M. Starch synthesis in amyloplasts purified from developing potato tubers. *Plant J.* **1997**, *11*, 1095–1103. [[CrossRef](#)]
3. Tanios, S.; Eyles, A.; Tegg, R.; Wilson, C. Potato tuber greening: A review of predisposing factors, management and future challenges. *Am. J. Potato Res.* **2018**, *95*, 248–257. [[CrossRef](#)]
4. Bergenstråhle, A.; Tillberg, E.; Jonsson, L. Regulation of glycoalkaloid accumulation in potato tuber discs. *J. Plant Physiol.* **1992**, *140*, 269–275. [[CrossRef](#)]
5. Grunenfelder, L.A.; Knowles, L.O.; Hiller, L.K.; Knowles, N.R. Glycoalkaloid Development during Greening of Fresh Market Potatoes (*Solanum tuberosum* L.). *J. Agric. Food Chem.* **2006**, *54*, 5847–5854. [[CrossRef](#)]
6. Okamoto, H.; Ducreux, L.J.; Allwood, J.W.; Hedley, P.E.; Wright, A.; Gururajan, V.; Terry, M.J.; Taylor, M.A. Light regulation of chlorophyll and glycoalkaloid biosynthesis during tuber greening of potato *S. tuberosum*. *Front. Plant Sci.* **2020**, *11*, 753. [[CrossRef](#)] [[PubMed](#)]
7. Xiong, Y.; Liu, X.; You, Q.; Han, L.; Shi, J.; Yang, J.; Cui, W.; Zhang, H.; Chao, Q.; Zhu, Y. Analysis of DNA methylation in potato tuber in response to light exposure during storage. *Plant Physiol. Biochem.* **2022**, *170*, 218–224. [[CrossRef](#)]
8. Itkin, M.; Heinig, U.; Tzfadia, O.; Bhide, A.; Shinde, B.; Cardenas, P.; Bocobza, S.; Unger, T.; Malitsky, S.; Finkers, R. Biosynthesis of antinutritional alkaloids in solanaceous crops is mediated by clustered genes. *Science* **2013**, *341*, 175–179. [[CrossRef](#)]
9. Nützmann, H.W.; Huang, A.; Osbourn, A. Plant metabolic clusters—from genetics to genomics. *New Phytol.* **2016**, *211*, 771–789. [[CrossRef](#)]
10. Qiao, Y.; Zhang, J.; Zhang, J.; Wang, Z.; Ran, A.; Guo, H.; Wang, D.; Zhang, J. Integrated RNA-seq and sRNA-seq analysis reveals miRNA effects on secondary metabolism in *Solanum tuberosum* L. *Mol. Genet. Genom.* **2017**, *292*, 37–52. [[CrossRef](#)]
11. Kobayashi, K.; Masuda, T. Transcriptional regulation of tetrapyrrole biosynthesis in *Arabidopsis thaliana*. *Front. Plant Sci.* **2016**, *7*, 1811. [[CrossRef](#)] [[PubMed](#)]
12. Kong, S.-G.; Okajima, K. Diverse photoreceptors and light responses in plants. *J. Plant Res.* **2016**, *129*, 111–114. [[CrossRef](#)] [[PubMed](#)]
13. Cheng, Y.-L.; Tu, S.-L. Alternative splicing and cross-talk with light signaling. *Plant Cell Physiol.* **2018**, *59*, 1104–1110. [[CrossRef](#)]
14. Kreslavski, V.D.; Los, D.A.; Schmitt, F.-J.; Zharmukhamedov, S.K.; Kuznetsov, V.V.; Allakhverdiev, S.I. The impact of the phytochromes on photosynthetic processes. *Biochim. Biophys. Acta Bioenerg.* **2018**, *1859*, 400–408. [[CrossRef](#)] [[PubMed](#)]
15. Petermann, J.B.; Morris, S.C. The spectral responses of chlorophyll and glycoalkaloid synthesis in potato tubers (*Solanum tuberosum*). *Plant Sci.* **1985**, *39*, 105–110. [[CrossRef](#)]
16. Percival, G. The influence of light upon glycoalkaloid and chlorophyll accumulation in potato tubers (*Solanum tuberosum* L.). *Plant Sci.* **1999**, *145*, 99–107. [[CrossRef](#)]
17. Wang, W.; Zhang, J.; Wang, D.; Tao, S.; Ji, Y.; Wu, B. Relation between light qualities and accumulation of steroidal glycoalkaloids as well as signal molecule in cell in potato tubers. *Acta Agron. Sin.* **2010**, *36*, 629–635. [[CrossRef](#)]
18. Andersen, T.G.; Barberon, M.; Geldner, N. Suberization—The second life of an endodermal cell. *Curr. Opin. Plant Biol.* **2015**, *28*, 9–15. [[CrossRef](#)]
19. Graça, J. Suberin: The biopolyester at the frontier of plants. *Front. Chem.* **2015**, *3*, 62. [[CrossRef](#)]
20. Tanios, S.; Thangavel, T.; Eyles, A.; Tegg, R.S.; Nichols, D.S.; Corkrey, R.; Wilson, C.R. Suberin deposition in potato periderm: A novel resistance mechanism against tuber greening. *New Phytol.* **2020**, *225*, 1273–1284. [[CrossRef](#)]
21. Cárdenas, P.D.; Sonawane, P.D.; Pollier, J.; Vanden Bossche, R.; Dewangan, V.; Weithorn, E.; Tal, L.; Meir, S.; Rogachev, I.; Malitsky, S. *GAME9* regulates the biosynthesis of steroidal alkaloids and upstream isoprenoids in the plant mevalonate pathway. *Nat. Commun.* **2016**, *7*, 10654. [[CrossRef](#)] [[PubMed](#)]
22. Sánchez-Retuerta, C.; Suárez-López, P.; Henriques, R. Under a new light: Regulation of light-dependent pathways by non-coding RNAs. *Front. Plant Sci.* **2018**, *9*, 962. [[CrossRef](#)]

23. Islam, W.; Waheed, A.; Idrees, A.; Rashid, J.; Zeng, F. Role of plant microRNAs and their corresponding pathways in fluctuating light conditions. *BBA-Mol. Cell Res.* **2022**, *1870*, 119304. [[CrossRef](#)] [[PubMed](#)]
24. Sun, W.; Xu, X.H.; Wu, X.; Wang, Y.; Lu, X.; Sun, H.; Xie, X. Genome-wide identification of microRNAs and their targets in wild type and phyB mutant provides a key link between microRNAs and the phyB-mediated light signaling pathway in rice. *Front. Plant Sci.* **2015**, *6*, 372. [[CrossRef](#)] [[PubMed](#)]
25. Martin, A.; Adam, H.; Díaz-Mendoza, M.; Zurczak, M.; González-Schain, N.D.; Suárez-López, P. Graft-transmissible induction of potato tuberization by the microRNA miR172. *Development* **2009**, *136*, 2873–2881. [[CrossRef](#)]
26. Folkes, L.; Moxon, S.; Woolfenden, H.C.; Stocks, M.B.; Szittyta, G.; Dalmay, T.; Moulton, V. PAREsnip: A tool for rapid genome-wide discovery of small RNA/target interactions evidenced through degradome sequencing. *Nucleic Acids Res.* **2012**, *40*, e103. [[CrossRef](#)]
27. Lin, S.S.; Chen, Y.; Lu, M.Y.J. Degradome Sequencing in Plants. In *Plant MicroRNAs. Methods in Molecular Biology*; Folter, S.D., Ed.; Humana Press: New York, NY, USA, 2019; Volume 1932, pp. 197–213.
28. Mweetwa, A.M.; Hunter, D.; Poe, R.; Harich, K.C.; Ginzberg, I.; Veilleux, R.E.; Tokuhisa, J.G. Steroidal glycoalkaloids in *Solanum chacoense*. *Phytochemistry* **2012**, *75*, 32–40. [[CrossRef](#)]
29. Murashige, T.; Skoog, F. A revised medium for rapid growth and bio assays with tobacco tissue cultures. *Physiol. Plant.* **1962**, *15*, 473–497. [[CrossRef](#)]
30. Kozomara, A.; Birgaoanu, M.; Griffiths-Jones, S. miRBase: From microRNA sequences to function. *Nucleic Acids Res.* **2019**, *47*, D155–D162. [[CrossRef](#)]
31. Brousse, C.; Liu, Q.; Beauclair, L.; Deremetz, A.; Axtell, M.J.; Bouche, N. A non-canonical plant microRNA target site. *Nucleic Acids Res.* **2014**, *42*, 5270–5279. [[CrossRef](#)]
32. McWilliam, H.; Li, W.; Uludag, M.; Squizzato, S.; Park, Y.M.; Buso, N.; Cowley, A.P.; Lopez, R. Analysis tool web services from the EMBL-EBI. *Nucleic Acids Res.* **2013**, *41*, W597–W600. [[CrossRef](#)]
33. Chen, C.; Chen, H.; Zhang, Y.; Thomas, H.R.; Frank, M.H.; He, Y.; Xia, R. TBtools: An integrative toolkit developed for interactive analyses of big biological data. *Mol. Plant* **2020**, *13*, 1194–1202. [[CrossRef](#)]
34. Kumar, L.; Futschik, M.E. Mfuzz: A software package for soft clustering of microarray data. *Bioinformatics* **2007**, *2*, 5. [[CrossRef](#)] [[PubMed](#)]
35. Oksanen, J.; Kindt, R.; Legendre, P.; O'Hara, B.; Stevens, M.H.H.; Oksanen, M.J.; Suggests, M. The vegan package. *Commun. Ecol. Pack.* **2007**, *10*, 631–637.
36. Varkonyi-Gasic, E.; Wu, R.; Wood, M.; Walton, E.F.; Hellens, R.P. Protocol: A highly sensitive RT-PCR method for detection and quantification of microRNAs. *Plant Methods* **2007**, *3*, 12. [[CrossRef](#)] [[PubMed](#)]
37. Varkonyi-Gasic, E. Stem-loop qRT-PCR for the detection of plant microRNAs. *Plant Epigenetics Methods Protoc.* **2017**, *1456*, 163–175.
38. Nicot, N.; Hausman, J.F.; Hoffmann, L.; Evers, D. Housekeeping gene selection for real-time RT-PCR normalization in potato during biotic and abiotic stress. *J. Exp. Bot.* **2005**, *56*, 2907–2914. [[CrossRef](#)]
39. Livak, K.J.; Schmittgen, T.D. Analysis of relative gene expression data using real-time quantitative PCR and the $2^{-\Delta\Delta CT}$ method. *Methods* **2001**, *25*, 402–408. [[CrossRef](#)]
40. Mao, J.; Mo, Z.; Yuan, G.; Xiang, H.; Visser, R.G.; Bai, Y.; Liu, H.; Wang, Q.; van der Linden, C.G. The CBL-CIPK network is involved in the physiological crosstalk between plant growth and stress adaptation. *Plant Cell Environ.* **2022**. Online ahead of print. [[CrossRef](#)]
41. Budak, H.; Kantar, M.; Bulut, R.; Akpinar, B.A. Stress responsive miRNAs and isomiRs in cereals. *Plant Sci.* **2015**, *235*, 1–13. [[CrossRef](#)]
42. Bhogireddy, S.; Mangrauthia, S.K.; Kumar, R.; Pandey, A.K.; Singh, S.; Jain, A.; Budak, H.; Varshney, R.K.; Kudapa, H. Regulatory non-coding RNAs: A new frontier in regulation of plant biology. *Funct. Integr. Genom.* **2021**, *21*, 313–330. [[CrossRef](#)]
43. Zhou, B.; Fan, P.; Li, Y.; Yan, H.; Xu, Q. Exploring miRNAs involved in blue/UV-A light response in *Brassica rapa* reveals special regulatory mode during seedling development. *BMC Plant Biol.* **2016**, *16*, 1–13. [[CrossRef](#)]
44. Zhou, X.; Wang, G.; Zhang, W. UV-B responsive microRNA genes in *Arabidopsis thaliana*. *Mol. Syst. Biol.* **2007**, *3*, 103. [[CrossRef](#)]
45. Foyer, C.H.; Rasool, B.; Davey, J.W.; Hancock, R.D. Cross-tolerance to biotic and abiotic stresses in plants: A focus on resistance to aphid infestation. *J. Exp. Bot.* **2016**, *67*, 2025–2037. [[CrossRef](#)] [[PubMed](#)]
46. Hossain, M.A.; Li, Z.-G.; Hoque, T.S.; Burritt, D.J.; Fujita, M.; Munné-Bosch, S. Heat or cold priming-induced cross-tolerance to abiotic stresses in plants: Key regulators and possible mechanisms. *Protoplasma* **2018**, *255*, 399–412. [[CrossRef](#)] [[PubMed](#)]
47. Fasani, E.; DalCorso, G.; Costa, A.; Zenoni, S.; Furini, A. The *Arabidopsis thaliana* transcription factor MYB59 regulates calcium signalling during plant growth and stress response. *Plant Mol. Biol.* **2019**, *99*, 517–534. [[CrossRef](#)] [[PubMed](#)]
48. Sabehat, A.; Weiss, D.; Lurie, S. Heat-shock proteins and cross-tolerance in plants. *Physiol. Plant.* **1998**, *103*, 437–441. [[CrossRef](#)]
49. Yang, F.; Qiao, Y.; Wang, Y.-Q.; Li, Q.; Li, D.; Wang, Y.-S.; Chai, W.-W. Genome-Wide Identification of HSP90 Genes and Expression Analysis under High Temperature and Drought Stresses in Potato. *Acta Agric. Boreali. Occident. Sin.* **2022**, *30*, 690–702.
50. Peng, J.; Li, Z.; Wen, X.; Li, W.; Shi, H.; Yang, L.; Zhu, H.; Guo, H. Salt-induced stabilization of EIN3/EIL1 confers salinity tolerance by deterring ROS accumulation in *Arabidopsis*. *PLoS Genet.* **2014**, *10*, e1004664. [[CrossRef](#)]
51. Pelletier, M.K.; Burbulis, I.E.; Winkel-Shirley, B. Disruption of specific flavonoid genes enhances the accumulation of flavonoid enzymes and end-products in *Arabidopsis* seedlings. *Plant Mol. Biol.* **1999**, *40*, 45–54. [[CrossRef](#)]

52. Kim, J.; Lee, W.J.; Vu, T.T.; Jeong, C.Y.; Hong, S.-W.; Lee, H. High accumulation of anthocyanins via the ectopic expression of *AtDFR* confers significant salt stress tolerance in *Brassica napus* L. *Plant Cell Rep.* **2017**, *36*, 1215–1224. [[CrossRef](#)] [[PubMed](#)]
53. Gao, F.; Robe, K.; Bettembourg, M.; Navarro, N.; Rofidal, V.; Santoni, V.; Gaymard, F.; Vignols, F.; Roschztardt, H.; Izquierdo, E. The transcription factor bHLH121 interacts with bHLH105 (ILR3) and its closest homologs to regulate iron homeostasis in Arabidopsis. *Plant Cell* **2020**, *32*, 508–524. [[CrossRef](#)] [[PubMed](#)]
54. Lei, R.; Li, Y.; Cai, Y.; Li, C.; Pu, M.; Lu, C.; Yang, Y.; Liang, G. *bHLH121* functions as a direct link that facilitates the activation of *FIT* by *bHLH IVc* transcription factors for maintaining Fe homeostasis in Arabidopsis. *Mol. Plant* **2020**, *13*, 634–649. [[CrossRef](#)] [[PubMed](#)]
55. Yu, Z.-X.; Wang, L.-J.; Zhao, B.; Shan, C.-M.; Zhang, Y.-H.; Chen, D.-F.; Chen, X.-Y. Progressive regulation of sesquiterpene biosynthesis in Arabidopsis and Patchouli (*Pogostemon cablin*) by the miR156-targeted *SPL* transcription factors. *Mol. Plant* **2015**, *8*, 98–110. [[CrossRef](#)]
56. Krits, P.; Fogelman, E.; Ginzberg, I. Potato steroidal glycoalkaloid levels and the expression of key isoprenoid metabolic genes. *Planta* **2007**, *227*, 143–150. [[CrossRef](#)]
57. Maya-Bernal, J.L.; Ávila, A.; Ruiz-Gayosso, A.; Trejo-Fregoso, R.; Pulido, N.; Sosa-Peinado, A.; Zúñiga-Sánchez, E.; Martínez-Barajas, E.; Rodríguez-Sotres, R.; Coello, P. Expression of recombinant *SnRK1* in *E. coli*. Characterization of adenine nucleotide binding to the *SnRK1. 1/AKINβγ-β3* complex. *Plant Sci.* **2017**, *263*, 116–125. [[CrossRef](#)]
58. Thelander, M.; Olsson, T.; Ronne, H. Snf1-related protein kinase 1 is needed for growth in a normal day–night light cycle. *EMBO J.* **2004**, *23*, 1900–1910. [[CrossRef](#)]
59. Ginzberg, I.; Thippeswamy, M.; Fogelman, E.; Demirel, U.; Mweetwa, A.M.; Tokuhisa, J.; Veilleux, R.E. Induction of potato steroidal glycoalkaloid biosynthetic pathway by overexpression of cDNA encoding primary metabolism HMG-CoA reductase and squalene synthase. *Planta* **2012**, *235*, 1341–1353. [[CrossRef](#)]

Disclaimer/Publisher’s Note: The statements, opinions and data contained in all publications are solely those of the individual author(s) and contributor(s) and not of MDPI and/or the editor(s). MDPI and/or the editor(s) disclaim responsibility for any injury to people or property resulting from any ideas, methods, instructions or products referred to in the content.